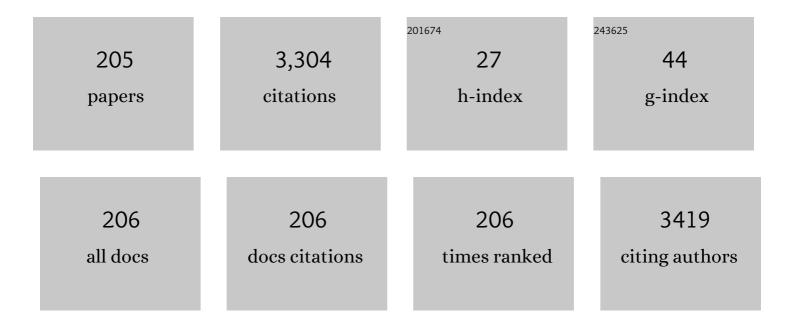
Naser M Ahmed

List of Publications by Year in descending order

Source: https://exaly.com/author-pdf/5457588/publications.pdf Version: 2024-02-01



#	Article	IF	CITATIONS
1	A wide-band UV photodiode based on n-ZnO/p-Si heterojunctions. Sensors and Actuators A: Physical, 2014, 207, 61-66.	4.1	114
2	Fabrication and characterization of V2O5 nanorods based metal–semiconductor–metal photodetector. Sensors and Actuators A: Physical, 2016, 250, 250-257.	4.1	98
3	A highly sensitive flexible SnS thin film photodetector in the ultraviolet to near infrared prepared by chemical bath deposition. RSC Advances, 2016, 6, 114980-114988.	3.6	96
4	The effect of post annealing temperature on grain size of indium-tin-oxide for optical and electrical properties improvement. Results in Physics, 2019, 13, 102159.	4.1	91
5	High sensitivity and fast response and recovery times in a ZnO nanorod array/ <i>p</i> -Si self-powered ultraviolet detector. Applied Physics Letters, 2012, 101, .	3.3	90
6	A high-sensitivity, fast-response, rapid-recovery UV photodetector fabricated based on catalyst-free growth of ZnO nanowire networks on glass substrate. Optical Materials, 2016, 60, 30-37.	3.6	82
7	High Sensitivity pH Sensor Based on Porous Silicon (PSi) Extended Gate Field-Effect Transistor. Sensors, 2016, 16, 839.	3.8	68
8	Synthesis and characterization of single-crystal CdS nanosheet for high-speed photodetection. Physica E: Low-Dimensional Systems and Nanostructures, 2012, 44, 1716-1721.	2.7	67
9	A high-sensitivity, fast-response, rapid-recovery p–n heterojunction photodiode based on rutile TiO2 nanorod array on p-Si(111). Applied Surface Science, 2014, 305, 445-452.	6.1	64
10	High performance near infrared photodetector based on cubic crystal structure SnS thin film on a glass substrate. Materials Letters, 2017, 200, 10-13.	2.6	59
11	Fabrication of low cost UV photo detector using ZnO nanorods grown onto nylon substrate. Journal of Materials Science: Materials in Electronics, 2015, 26, 1322-1331.	2.2	57
12	UV photodetector behavior of 2D ZnO plates prepared by electrochemical deposition. Superlattices and Microstructures, 2012, 51, 765-771.	3.1	50
13	High performance CuS p-type thin film as a hydrogen gas sensor. Sensors and Actuators A: Physical, 2016, 249, 68-76.	4.1	50
14	High performance and low-cost UV–Visible–NIR photodetector based on tin sulphide nanostructures. Journal of Alloys and Compounds, 2018, 735, 2256-2262.	5.5	50
15	Structural and optical investigations of cadmium sulfide nanostructures for optoelectronic applications. Solar Energy, 2012, 86, 3234-3240.	6.1	47
16	Ag/ZnO/p-Si/Ag heterojunction and their optoelectronic characteristics under different UV wavelength illumination. Sensors and Actuators A: Physical, 2016, 242, 50-57.	4.1	47
17	Self-assembly of aligned CuO nanorod arrays using nanoporous anodic alumina template by electrodeposition on Si substrate for IR photodetectors. Sensors and Actuators A: Physical, 2016, 239, 209-219.	4.1	46
18	Effect of substrate temperature on indium tin oxide (ITO) thin films deposited by jet nebulizer spray pyrolysis and solar cell application. Materials Science in Semiconductor Processing, 2014, 27, 562-568.	4.0	45

#	Article	IF	CITATIONS
19	Growth of vertically aligned ZnO nanorods on Teflon as a novel substrate for low-power flexible light sensors. Applied Physics A: Materials Science and Processing, 2015, 119, 1197-1201.	2.3	45
20	Fabrication and characterization of nanocrystalline CdS thin film-based optical sensor grown via microwave-assisted chemical bath deposition. Superlattices and Microstructures, 2014, 67, 8-16.	3.1	43
21	Growth and characterization of CdS single-crystalline micro-rod photodetector. Superlattices and Microstructures, 2013, 54, 137-145.	3.1	40
22	Fabrication of a highly flexible low-cost H2 gas sensor using ZnO nanorods grown on an ultra-thin nylon substrate. Journal of Materials Science: Materials in Electronics, 2016, 27, 9461-9469.	2.2	38
23	Effects of ZnO seed layer thickness on catalyst-free growth of ZnO nanostructures for enhanced UV photoresponse. Optics and Laser Technology, 2018, 98, 344-353.	4.6	37
24	Effect of nano zinc oxide and silica on mechanical, fluid transport and radiation attenuation properties of steel furnace slag heavyweight concrete. Construction and Building Materials, 2021, 274, 121785.	7.2	34
25	Fabrication and characterization of ZnO thin film using sol–gel method. Optik, 2013, 124, 491-492.	2.9	33
26	A study of the effects of aligned vertically growth time on ZnO nanorods deposited for the first time on Teflon substrate. Applied Surface Science, 2017, 426, 906-912.	6.1	33
27	Influence of CuS membrane annealing time on the sensitivity of EGFET pH sensor. Materials Science in Semiconductor Processing, 2017, 71, 217-225.	4.0	30
28	Influence of pH value on structural, optical and photoresponse properties of SnS films grown via chemical bath deposition. Materials Letters, 2018, 210, 279-282.	2.6	30
29	Influences of substrate type on the pH sensitivity of CuS thin films EGFET prepared by spray pyrolysis deposition. Materials Science in Semiconductor Processing, 2017, 63, 269-278.	4.0	28
30	Areca catechu extracted natural new sensitizer for dye-sensitized solar cell: performance evaluation. Journal of Materials Science: Materials in Electronics, 2020, 31, 3564-3575.	2.2	28
31	ZnO nanofiber (NFs) growth from ZnO nanowires (NWs) by controlling growth temperature on flexible Teflon substrate by CBD technique for UV photodetector. Superlattices and Microstructures, 2016, 100, 1120-1127.	3.1	27
32	Effects of ammonia-ambient annealing on physical and electrical characteristics of rare earth CeO2 as passivation film on silicon. Journal of Alloys and Compounds, 2017, 695, 3104-3115.	5.5	27
33	A Study on the UV Photoresponse of Hydrothermally Grown Zinc Oxide Nanorods With Different Aspect Ratios. IEEE Sensors Journal, 2015, 15, 6811-6818.	4.7	26
34	High-performance p–n heterojunction photodetectors based on V2O5 nanorods by spray pyrolysis. Applied Physics A: Materials Science and Processing, 2016, 122, 1.	2.3	26
35	Effects of the voltage and time of anodization on modulation of the pore dimensions of AAO films for nanomaterials synthesis. Superlattices and Microstructures, 2015, 88, 489-500.	3.1	25
36	Effects of CW CO ₂ Laser Annealing on Indium Tin Oxide Thin Films Characteristics. Soft Nanoscience Letters, 2014, 04, 83-89.	0.8	25

#	Article	IF	CITATIONS
37	Characteristics of Extended-Gate Field-Effect Transistor (EGFET) Based on Porous n-Type (111) Silicon for Use in pH Sensors. Journal of Electronic Materials, 2017, 46, 5804-5813.	2.2	24
38	Effect of Annealing Time of YAG:Ce3+ Phosphor on White Light Chromaticity Values. Journal of Electronic Materials, 2018, 47, 1638-1646.	2.2	24
39	Green synthesis of zinc oxide nanoparticles using salvia officials extract. Materials Science in Semiconductor Processing, 2021, 125, 105641.	4.0	24
40	Catalyst-free growth of ZnO nanowires on ITO seed layer/glass by thermal evaporation method: Effects of ITO seed layer laser annealing temperature. Superlattices and Microstructures, 2016, 92, 68-79.	3.1	23
41	Control of Phase, Structural and Optical Properties of Tin Sulfide Nanostructured Thin Films Grown via Chemical Bath Deposition. Journal of Electronic Materials, 2017, 46, 4227-4235.	2.2	23
42	Physicomechanical and gamma-ray shielding properties of high-strength heavyweight concrete containing steel furnace slag aggregate. Journal of Building Engineering, 2020, 30, 101306.	3.4	23
43	Numerical Modelling Analysis for Carrier Concentration Level Optimization of CdTe Heterojunction Thin Film–Based Solar Cell with Different Non–Toxic Metal Chalcogenide Buffer Layers Replacements: Using SCAPS–1D Software. Crystals, 2021, 11, 1454.	2.2	23
44	Fabrication and characterization of nanocrystalline n-CdO/p-Si as a solar cell. Superlattices and Microstructures, 2012, 52, 800-806.	3.1	22
45	Structural, Analysis and Optical Studies of Cadmium Sulfide Nanostructured. Procedia Engineering, 2013, 53, 217-224.	1.2	22
46	Effect of Annealing on the Electrical Properties of CuxS Thin Films. Procedia Chemistry, 2016, 19, 15-20.	0.7	22
47	Comprehensive photoresponse study on high performance and flexible π-SnS photodetector with near-infrared response. Materials Science in Semiconductor Processing, 2019, 100, 270-274.	4.0	22
48	Effects of annealing on the optical and electrical properties of CdO thin films prepared by thermal evaporation. Materials Letters, 2013, 105, 84-86.	2.6	21
49	High sensitivity extended gate effect transistor based on V2O5 nanorods. Journal of Materials Science: Materials in Electronics, 2017, 28, 1364-1369.	2.2	21
50	Impact of ablation time on Cu oxide nanoparticle green synthesis via pulsed laser ablation in liquid media. Applied Physics A: Materials Science and Processing, 2018, 124, 1.	2.3	21
51	A novel porous silicon multi-ions selective electrode based extended gate field effect transistor for sodium, potassium, calcium, and magnesium sensor. Applied Physics A: Materials Science and Processing, 2019, 125, 1.	2.3	21
52	Ultraviolet electroluminescence from flowers-like n-ZnO nanorods/p-GaN light-emitting diode fabricated by modified chemical bath deposition. Journal of Luminescence, 2020, 226, 117510.	3.1	21
53	Characterization of V2O5 nanorods grown by spray pyrolysis technique. Journal of Materials Science: Materials in Electronics, 2016, 27, 4613-4621.	2.2	20
54	Study of the structural and luminescent properties of Ce3+ and Eu3+ co-doped YAG synthesized by solid state reaction. Optik, 2018, 158, 152-163.	2.9	20

#	Article	IF	CITATIONS
55	Engineering and gamma-ray attenuation properties of steel furnace slag heavyweight concrete with nano calcium carbonate and silica. Construction and Building Materials, 2021, 267, 120878.	7.2	20
56	Modern heavyweight concrete shielding: Principles, industrial applications and future challenges; review. Journal of Building Engineering, 2021, 39, 102290.	3.4	20
57	Fabrication and characterization of ZnO nanowires by wet oxidation of Zn thin film deposited on Teflon substrate. Superlattices and Microstructures, 2015, 86, 236-242.	3.1	19
58	Erythrocyte sedimentation rate of human blood exposed to low-level laser. Lasers in Medical Science, 2016, 31, 1195-1201.	2.1	19
59	Low-power UV photodetection characteristics of ZnO tetrapods grown on catalyst-free glass substrate. Sensors and Actuators A: Physical, 2016, 250, 187-194.	4.1	18
60	Sensitivity of CuS and CuS/ITO EGFETs implemented as pH sensors. Applied Physics A: Materials Science and Processing, 2016, 122, 1.	2.3	18
61	Large-scale uniform ZnO tetrapods on catalyst free glass substrate by thermal evaporation method. Materials Research Bulletin, 2016, 79, 63-68.	5.2	18
62	Flexible low–cost infrared photodetector based on SnS thin film grown by chemical bath deposition. Materials Research Express, 2017, 4, 105033.	1.6	18
63	Dependence of pH on phase stability, optical and photoelectrical properties of SnS thin films. Superlattices and Microstructures, 2019, 128, 170-176.	3.1	18
64	ZnO quantum dot based thin films as promising electron transport layer: Influence of surface-to-volume ratio on the photoelectric properties. Ceramics International, 2021, 47, 12397-12409.	4.8	18
65	Fabrication and Characterization of 50 nm Silicon Nano-Gap Structures. Science of Advanced Materials, 2011, 3, 233-238.	0.7	18
66	GaN Schottky barrier photodiode on Si (111) with low-temperature-grown cap layer. Journal of Alloys and Compounds, 2009, 481, L15-L19.	5.5	17
67	Nano and micro porous GaN characterization using image processing method. Optik, 2012, 123, 1074-1078.	2.9	17
68	Effect of Sn doping and annealing on the morphology, structural, optical, and electrical properties of 3D (micro/nano) V2O5 sphere for high sensitivity pH-EGFET sensor. Sensors and Actuators B: Chemical, 2020, 305, 127515.	7.8	17
69	AlN/GaN/AlN heterostructures grown on Si substrate by plasma-assisted MBE for MSM UV photodetector applications. Materials Science in Semiconductor Processing, 2015, 29, 231-237.	4.0	16
70	Responsivity Dependent Anodization Current Density of Nanoporous Silicon Based MSM Photodetector. Journal of Nanomaterials, 2016, 2016, 1-8.	2.7	16
71	Multilayer ZnO/Pd/ZnO Structure as Sensing Membrane for Extended-Gate Field-Effect Transistor (EGFET) with High pH Sensitivity. Journal of Electronic Materials, 2017, 46, 5901-5908.	2.2	16
72	Electrochemical Hydrogen Peroxide Sensor Based on Macroporous Silicon. Sensors, 2018, 18, 716.	3.8	16

#	Article	IF	CITATIONS
73	Effect of gamma irradiation dose on the structure and pH sensitivity of ITO thin films in extended gate field effect transistor. Results in Physics, 2019, 12, 615-622.	4.1	16
74	Hydrogen gas sensor based on nanofibers TiO2-PVP thin film at room temperature prepared by electrospinning. Microsystem Technologies, 2021, 27, 293-299.	2.0	16
75	Fast UV detection and hydrogen sensing by ZnO nanorod arrays grown on a flexible Kapton tape. Materials Science-Poland, 2013, 31, 180-185.	1.0	15
76	Preparation of thin hexagonal highly-ordered anodic aluminum oxide (AAO) template onto silicon substrate and growth ZnO nanorod arrays by electrodeposition. Superlattices and Microstructures, 2014, 76, 197-204.	3.1	15
77	Effect of Substrate on the Photodetection Characteristics of ZnO-PAni Composites. ECS Journal of Solid State Science and Technology, 2016, 5, P305-P308.	1.8	15
78	A novel CuS thin film deposition method by laser-assisted spray photolysis deposition and its application to EGFET. Sensors and Actuators B: Chemical, 2017, 247, 197-215.	7.8	15
79	Fabrication, characterization of ZnO nanorods on the flexible substrate (Kapton tape) via chemical bath deposition for UV photodetector applications. AIP Conference Proceedings, 2017, , .	0.4	15
80	pn-Junction photodiode based on GaN grown on Si (111) by plasma-assisted molecular beam epitaxy. Materials Science in Semiconductor Processing, 2013, 16, 1859-1864.	4.0	14
81	Preparation of CuO nanoparticles by laser ablation in liquid. AIP Conference Proceedings, 2016, , .	0.4	14
82	Laser-induced solution combustion of nano-Y 2.96 Al 5 O 12 :0.04Ce phosphors and their fluorescent properties for white light conversion. Journal of Alloys and Compounds, 2017, 711, 42-50.	5.5	14
83	Investigation of sintering temperature and Ce3+ concentration in YAG:Ce phosphor powder prepared by microwave combustion for white-light-emitting diode luminance applications. Materials Chemistry and Physics, 2019, 229, 22-31.	4.0	14
84	A high-performance near-infrared photodetector based on π-SnS phase. Materials Letters, 2020, 273, 127910.	2.6	14
85	Properties of NiO nanostructured growth using thermal dry oxidation of nickel metal thin film for hydrogen gas sensing at room temperature. Materials Research Express, 2017, 4, 075009.	1.6	13
86	Sensitivity of CuS Membrane pH Sensor With and Without MOSFET. Jom, 2017, 69, 1134-1142.	1.9	13
87	Low-Intensity UV light sensor based on p-NiO/n-Si heterojunction. Materials Research Express, 2019, 6, 126332.	1.6	13
88	Development of EGFET-based ITO pH sensors using epoxy free membrane. Semiconductor Science and Technology, 2021, 36, 045027.	2.0	13
89	Characteristics of Nanostructure Silicon Photodiode using Laser Assisted Etching. Procedia Engineering, 2013, 53, 393-399.	1.2	12
90	Catalytic growth of one-dimensional single-crystalline ZnO nanostructures on glass substrate by vapor transport. Ceramics International, 2017, 43, 610-616.	4.8	12

#	Article	IF	CITATIONS
91	Synthesis of quantum dot porous silicon as extended gate field effect transistor (EGFET) for a pH sensor application. Materials Science in Semiconductor Processing, 2019, 100, 167-174.	4.0	12
92	Rapid synthesis of Ce3+:YAG via CO2 laser irradiation combustion method: Influence of Ce doping and thickness of phosphor ceramic on the performance of a white LED device. Journal of Solid State Chemistry, 2021, 294, 121866.	2.9	12
93	Effect of Deposition Temperature on Structural and Optical Properties of Chemically Sprayed ZnS Thin Films. Procedia Chemistry, 2016, 19, 485-491.	0.7	11
94	High Responsivity IR Photodetector Based on CuO Nanorod Arrays/AAO Assembly. Procedia Chemistry, 2016, 19, 311-318.	0.7	11
95	Porous Formation in p-Type Gallium Nitride Films via 50ÂHz Operated Alternating Current-Assisted Photo-Electrochemical Etching in Methanol-Sulfuric Acid Solution. Journal of the Electrochemical Society, 2018, 165, H620-H628.	2.9	11
96	Growth of ZnS Thin Films using Chemical Spray Pyrolysis Technique. Materials Today: Proceedings, 2019, 17, 912-920.	1.8	11
97	Effect of Addition of Polyaniline on Polyethylene Oxide and Polyvinyl Alcohol for the Fabrication of Nanorods. ACS Omega, 2020, 5, 22389-22394.	3.5	11
98	Study of acidosis, neutral and alkalosis media effects on the behaviour of activated carbon threads decorated by zinc oxide using extended gate FET for glucose sensor application. Materials Science in Semiconductor Processing, 2020, 108, 104911.	4.0	11
99	Synthesis & thermoluminescence characteristics & structural and optical studies of ZnO/Ag/ZnO system for dosimetric applications. Journal of Luminescence, 2021, 236, 118097.	3.1	11
100	Characterization of porous silicon thin films passivated by a nano-silver layer. Materials Science in Semiconductor Processing, 2015, 31, 235-239.	4.0	10
101	UV sensing of twinned ZnO–PANI composite. Applied Physics A: Materials Science and Processing, 2016, 122, 1.	2.3	10
102	Surface Alteration of Planar P-Type Gallium Nitride to Porous Structure Using 50 Hz Alternating Current-Assisted Photo-Electrochemical Etching Route. Journal of the Electrochemical Society, 2016, 163, H642-H651.	2.9	10
103	Ag metal mid layer based on new sensing multilayers structure extended gate field effect transistor (EG-FET) for pH sensor. Materials Science in Semiconductor Processing, 2018, 74, 51-56.	4.0	10
104	Single- and double-thread activated carbon fibers for pH sensing. Materials Chemistry and Physics, 2019, 221, 288-294.	4.0	10
105	Ce-doped YAG single-crystals prepared by continuous wave (CW)–CO2 laser combustion technique with attractive characteristics and moderate white LED performance. Optics and Laser Technology, 2020, 132, 106506.	4.6	10
106	Broadband visible emission from photoelectrochemical etched porous silicon quantum dots containing zinc. Materials Chemistry and Physics, 2021, 258, 123935.	4.0	10
107	Structural and optical properties of PbI2 nanostructures obtained using the thermal evaporation method. Canadian Journal of Physics, 2013, 91, 826-832.	1.1	9
108	Influence of wet etching time cycles on morphology features of thin porous Anodic Aluminum oxide (AAO) template for nanostructure's synthesis. Journal of Physics and Chemistry of Solids, 2015, 87, 1-8.	4.0	9

#	Article	IF	CITATIONS
109	Influence of solution deposition rate on properties of V2O5 thin films deposited by spray pyrolysis technique. AIP Conference Proceedings, 2016, , .	0.4	9
110	Effects of low-level laser irradiation on human blood lymphocytes in vitro. Lasers in Medical Science, 2017, 32, 405-411.	2.1	9
111	Sputtered growth of high mobility InN thin films on different substrates using Cu-ZnO buffer layer. Materials Science in Semiconductor Processing, 2017, 71, 166-173.	4.0	9
112	Tin Sulfide Flower-Like Structure as High-Performance Near-Infrared Photodetector. Journal of Electronic Materials, 2020, 49, 5824-5830.	2.2	9
113	Synthesis ZnO nanoclusters micro active area using continues wave blue laser-assisted chemical bath deposition based on UV photodetector. Optik, 2022, 260, 169099.	2.9	9
114	Laser-induced changes of in vitro erythrocyte sedimentation rate. Lasers in Medical Science, 2017, 32, 2089-2095.	2.1	8
115	Hydrothermal and solvothermal synthesis of nanorods and 3D (micro/nano) V2O5 on macro PSi substrate for pH-EGFET sensors. Journal of Materials Science: Materials in Electronics, 2019, 30, 11193-11207.	2.2	8
116	White, blue and green emission from Si QDs derived from zinc incorporated porous silicon. Journal of Luminescence, 2021, 232, 117845.	3.1	8
117	Effect of nano-silica slurry on engineering, X-ray, and γ-ray attenuation characteristics of steel slag high-strength heavyweight concrete. Nanotechnology Reviews, 2020, 9, 1245-1264.	5.8	8
118	ZnO Nanorods/Polyaniline-Based Inorganic/Organic Heterojunctions for Enhanced Light Sensing Applications. ECS Journal of Solid State Science and Technology, 2016, 5, P142-P147.	1.8	7
119	A comparative study of InN growth on quartz, silicon, C-sapphire and bulk GaN substrates by RF magnetron sputtering. Journal of Materials Science: Materials in Electronics, 2017, 28, 9228-9236.	2.2	7
120	Photo-electrochemically synthesized light emtting nanoporous silicon based UV photodetector: influence of current density. Materials Research Express, 2017, 4, 116203.	1.6	7
121	Effects of Concentration and Substrate Type on Structure and Conductivity of p-Type CuS Thin Films Grown by Spray Pyrolysis Deposition. Journal of Electronic Materials, 2017, 46, 218-225.	2.2	7
122	High-performance nanoporous silicon-based photodetectors. Optik, 2018, 168, 424-431.	2.9	7
123	Influence of growth temperature and duration on different properties of ultra-long ZnO nanorods grown by modified chemical bath deposition method. Materials Research Express, 2018, 5, 095020.	1.6	7
124	Catalytic Growth of 1D ZnO Nanoneedles on Glass Substrates Through Vapor Transport. Journal of Electronic Materials, 2019, 48, 1660-1668.	2.2	7
125	Multilayer ZnO/Pb/G thin film based extended gate field effect transistor for low dose gamma irradiation detection. Nuclear Instruments and Methods in Physics Research, Section A: Accelerators, Spectrometers, Detectors and Associated Equipment, 2021, 987, 164833.	1.6	7
126	Photoconversion efficiency of In2S3/ZnO core-shell heterostructures nanorod arrays deposited via controlled SILAR cycles. Heliyon, 2022, 8, e09959.	3.2	7

#	Article	IF	CITATIONS
127	Controllable fabrication of highly ordered thin AAO template on Si substrate for electrodeposition of nanostructures. Applied Physics A: Materials Science and Processing, 2014, 116, 1389-1393.	2.3	6
128	Control growth of catalyst-free ZnO tetrapods on glass substrate by thermal evaporation method. Ceramics International, 2016, 42, 13144-13150.	4.8	6
129	One-Step Synthesis of Stable Colloidal Gold Nanoparticles Through Bioconjugation with Bovine Serum Albumin in Harsh Environments. Journal of Cluster Science, 2017, 28, 3193-3207.	3.3	6
130	Optical and structural properties of curcuminoids extracted from Curcuma longa L. for hybrid white light diode. EPJ Applied Physics, 2018, 84, 10501.	0.7	6
131	Hydrothermal Synthesis and Structural Properties of V2O5 Nanoflowers at Low Temperatures. Journal of Physics: Conference Series, 2018, 1083, 012036.	0.4	6
132	Conductometric Gas Sensing Based on ZnO Thin Films: An Impedance Spectroscopy Study. ECS Journal of Solid State Science and Technology, 2018, 7, P487-P490.	1.8	6
133	Low power consumption UV sensor based on n-ZnO/p-Si junctions. Journal of Materials Science: Materials in Electronics, 2019, 30, 19639-19646.	2.2	6
134	Thermal evaporation based V ₂ O ₅ thin film for extended gate field effect transistor pH sensor. Materials Research Express, 2019, 6, 125423.	1.6	6
135	UV Photodetector Based on p-NiO film/n-Si Heterojunction Prepared by Thermal Oxidation. Journal of Physics: Conference Series, 2020, 1535, 012001.	0.4	6
136	Silicon quantum dot/black silicon hybrid nanostructure for broadband reflection reduction. Materials Science in Semiconductor Processing, 2020, 115, 105113.	4.0	6
137	Amperometric room temperature hydrogen gas sensor based on the conjugated polymers of polypyrrole–polyethylene oxide nanofibers synthesised via electrospinning. Journal of Materials Science: Materials in Electronics, 2022, 33, 7068-7078.	2.2	6
138	pH sensor based on AuNPs/ ITO membrane as extended gate field-effect transistor. Applied Physics B: Lasers and Optics, 2022, 128, 1.	2.2	6
139	Applications of the image processing method on the structure measurements in porous GaN. Journal of Experimental Nanoscience, 2014, 9, 87-95.	2.4	5
140	Influence of the spray distance to substrate on optical properties of chemically sprayed ZnS thin films. Journal of Materials Science: Materials in Electronics, 2017, 28, 371-375.	2.2	5
141	Atomistic modeling of InGaN/GaN quantum dots-in-nanowire for graded surface-emitting low-threshold, blue exciton laser. Results in Physics, 2021, 20, 103732.	4.1	5
142	The effect of deposition angle on morphology and diameter of electrospun TiO ₂ /PVP nanofibers. Nanocomposites, 2021, 7, 70-78.	4.2	5
143	Porous silicon based violet-UV detector. , 2012, , .		4
144	A Study of Properties of the Nanocrystalline CdO Thin Film Prepared by Solid-Vapor Deposition Method. Materials Science Forum, 0, 756, 54-58.	0.3	4

#	Article	IF	CITATIONS
145	The correlation of blue shift of photoluminescence and morphology of silicon nanoporous. AIP Conference Proceedings, 2016, , .	0.4	4
146	The Effect of the Annealing on the Properties of ZnO/Cu/ZnO Multilayer Structures. Procedia Chemistry, 2016, 19, 38-44.	0.7	4
147	Catalyst-free growth of ZnO nanowires on ITO seed/glass by thermal evaporation method: Effects of ITO seed layer thickness. AIP Conference Proceedings, 2016, , .	0.4	4
148	Growth mechanism of seed/catalyst-free zinc oxide nanowire balls using intermittently pumped carrier gas: Synthesis, characterization and applications. Optical Materials, 2017, 67, 70-77.	3.6	4
149	Effects of low power violet laser irradiation on red blood cells volume and erythrocyte sedimentation rate in human blood. AIP Conference Proceedings, 2017, , .	0.4	4
150	Structural, Electrical and Optical Properties of Sputtered-Grown InN Films on ZnO Buffered Silicon, Bulk GaN, Quartz and Sapphire Substrates. Journal of Electronic Materials, 2018, 47, 4875-4881.	2.2	4
151	Photovoltaic Performance of Spherical TiO2 Nanoparticles Derived from Titanium Hydroxide Ti(OH)4: Role of Annealing Varying Temperature. Energies, 2022, 15, 1648.	3.1	4
152	Ionization Radiation Shielding Effectiveness of Lead Acetate, Lead Nitrate, and Bismuth Nitrate-Doped Zinc Oxide Nanorods Thin Films: A Comparative Evaluation. Materials, 2022, 15, 3.	2.9	4
153	Structural and Morphological Studies of Cadmium Sulfide Nanostructures. Advanced Materials Research, 0, 795, 228-232.	0.3	3
154	INFLUENCE OF ANNEALING DURATION ON THE GROWTH OF V2O5 NANORODS SYNTHESIZED BY SPRAY PYROLYSIS TECHNIQUE. Surface Review and Letters, 2016, 23, 1650057.	1.1	3
155	Optimum Annealing Temperature for Transformation of NiO Nanoflakes from Chemically Grown Ni(OH) ₂ Nanostructure Thin Film. Journal of Nano Research, 0, 49, 75-84.	0.8	3
156	The Effect of The Wavelength of the LED used to Pump Phosphor Produced from Curcuminoids Dye Extracted from Turmeric (Curcuma Longa L.) to Produce White Light. IOP Conference Series: Materials Science and Engineering, 0, 454, 012048.	0.6	3
157	Characterization of nickel/indium tin oxide based extended gate-field effect transistor as glucose sensor in acidosis, normal and alkalosis media. Materials Science in Semiconductor Processing, 2019, 103, 104626.	4.0	3
158	EBT3 Films in Low Solar Ultraviolet and X-Ray Dose Measurement: A Comparative Analysis. Dose-Response, 2019, 17, 155932581985553.	1.6	3
159	Optimization of Precursor Concentration for the Fabrication of V2O5 Nanorods and their MSM Photodetector on Silicon Substrate. Journal of Electronic Materials, 2019, 48, 5640-5649.	2.2	3
160	AAO-Assisted Synthesis of Aligned CuO Nanorod Arrays by Electrochemical Deposition for Self-powered NIR Photodetection. Journal of Electronic Materials, 2019, 48, 7465-7473.	2.2	3
161	Structural and Optical Properties of Nanofibers Prepared with Electrospinning by Using PMMA Integrated with Curcuminoids to Produce White LED. Fibers and Polymers, 2020, 21, 1733-1742.	2.1	3
162	IMPROVEMENT IN STRUCTURAL, OPTICAL AND ELECTRICAL PROPERTIES OF ITO FILM THROUGH AIN AND HfO ₂ BUFFER LAYERS. Surface Review and Letters, 2021, 28, .	1.1	3

#	Article	IF	CITATIONS
163	ZnO Nanorods/Polyaniline Heterojunction onto SiO2 for Photosensor. Journal of Nanoelectronics and Optoelectronics, 2018, 13, 1034-1040.	0.5	3
164	Fabrication and Characterization of Gold Nano-gaps for ssDNA Immobilization and Hybridization Detection. Journal of New Materials for Electrochemical Systems, 2011, 14, 191-196.	0.6	3
165	Effect of thermal annealing on GaN pn-junction diode with Pt/Ag as ohmic contact. Composite Interfaces, 2014, 21, 371-380.	2.3	2
166	Structural Properties of PbI ₂ Thin Film. Advanced Materials Research, 0, 879, 175-179.	0.3	2
167	CuS p- type thin film characterization deposited on Ti, ITO and glass substrates using spray pyrolysis deposition (SPD) for light emitting diode (LED) application. AIP Conference Proceedings, 2016, , .	0.4	2
168	In vitro effects of low level yellow laser irradiation on human red blood cells. , 2016, , .		2
169	Simulation of optimum parameters for GaN MSM UV photodetector. AIP Conference Proceedings, 2016, , \cdot	0.4	2
170	Room temperature hydrogen gas sensing characteristics of porous quaternary AlInGaN film prepared via UV-assisted photo-electrochemical etching. Superlattices and Microstructures, 2016, 95, 65-70.	3.1	2
171	Using Deionized Water with Ethanol as a Solvent of CuS EGFET as pH Sensor. Materials Science Forum, 2017, 886, 37-41.	0.3	2
172	Structural, Electrical and Optical Properties of NiO Nanostructured Growth Using Thermal Wet Oxidation of Nickel Metal Thin Film. Journal of Nano Research, 2017, 49, 56-65.	0.8	2
173	pH Sensing Characteristics of CuS/ZnO Thin Film Implemented as EGFET. Journal of Physics: Conference Series, 2018, 1083, 012055.	0.4	2
174	Enhancement of Temperature Fluorescence Brightness of Zn@Si Core-Shell Quantum Dots Produced via a Unified Strategy. Nanomaterials, 2021, 11, 3158.	4.1	2
175	Improvement of Porous GaN-Based UV Photodetector with Graphene Cladding. Applied Sciences (Switzerland), 2021, 11, 10833.	2.5	2
176	Formation of titanium dioxide/poly(vinylpyrrolidone) nanostructure composite by changing the flow rate of polymer solution during electrospinning. Bulletin of Materials Science, 2022, 45, .	1.7	2
177	High sensitive UV photodetector based on ZnS/PS thin film prepared via spray pyrolysis method. Energy Sources, Part A: Recovery, Utilization and Environmental Effects, 2022, 44, 5303-5313.	2.3	2
178	Temperature Variation Effects on Current-Voltage (i-v) Characteristics of n-GaN Schottky Diode. Materials Science Forum, 2006, 517, 141-146.	0.3	1
179	EFFECT OF ETCHING TIME ON OPTICAL AND MORPHOLOGICAL FEATURES OF N-TYPE POROUS SILICON PREPARED BY PHOTO-ELECTROCHEMICAL METHOD. Jurnal Teknologi (Sciences and Engineering), 2016, 78, .	0.4	1
180	Novel nanorods based on PANI / PEO polymers using electrospinning method. AIP Conference Proceedings, 2016, , .	0.4	1

#	Article	IF	CITATIONS
181	Hydrothermal growth and characterization of vertically well-aligned and dense ZnO nanorods on glass and silicon using a simple optimizer system. AIP Conference Proceedings, 2016, , .	0.4	1
182	Growth and characterization of V2O5 nanorods deposited by spray pyrolysis at low temperatures. AIP Conference Proceedings, 2016, , .	0.4	1
183	Experimental investigation of unique color-changing property of multicolored sparkling of microbubbles formed due to femtosecond laser–water interaction. Modern Physics Letters B, 2019, 33, 1950208.	1.9	1
184	Enhanced white light luminescence of Ce3+ - activated Y3Al5O12 phosphors powder synthesized via continuous wave (CW) CO2 laser-assisted combustion. , 2019, , .		1
185	Fabrication and Characterization of Light Emitting Diode Based on n-ZnO Nanorods Grown Via a Low-Temperature. Journal of Physics: Conference Series, 2020, 1535, 012009.	0.4	1
186	Investigation on the characteristics of ZnO and ZnO-Pb structure for gamma radiation detection. Journal of Physics: Conference Series, 2020, 1535, 012028.	0.4	1
187	Innovative Approaches to Synthesize Novel Graphene Materials. Current Nanoscience, 2021, 17, .	1.2	1
188	Effect of sulphuric acid (H2SO4) on the growth process of two-dimensional zinc oxide (ZnO) structures prepared by chemical bath deposition. Applied Physics A: Materials Science and Processing, 2021, 127, 1.	2.3	1
189	Extended Gate Field Effect Transistor-Based N-Type Gallium Nitride as a pH Sensor. Journal of Electronic Materials, 2021, 50, 7071-7077.	2.2	1
190	Structural, Morphological and Optical Properties of V ₂ O ₅ Nanorods Grown Using Spray Pyrolysis Technique at Different Substrate Temperature. Nanoscience and Nanotechnology Letters, 2016, 8, 181-186.	0.4	1
191	Investigation of X-ray Radiation Detectability Using Fabricated ZnO-PB Based Extended Gate Field-Effect Transistor as X-ray Dosimeters. Applied Sciences (Switzerland), 2021, 11, 11258.	2.5	1
192	Sensitivity of Nickel Oxide Nanoflakes Layer on Extend Gate Field Effect Transistor for pH Sensor. Springer Proceedings in Complexity, 2021, , 303-313.	0.3	1
193	Optimization of InGaN Based Light Emitting Diodes. Materials Science Forum, 2006, 517, 195-201.	0.3	0
194	Effects of Layer Thickness and Incident Angle Variations on DBR Reflectivity. Materials Science Forum, 2006, 517, 29-32.	0.3	0
195	Concentration Effects on n-GaN Schottky Diode Current-Voltage (i-v) Characteristics. Materials Science Forum, 2006, 517, 159-164.	0.3	Ο
196	Design of DBR Mirrors for GaN Vertical Cavity Surface Emitting Laser. Materials Science Forum, 2006, 517, 25-28.	0.3	0
197	Light Extraction from GaN-Microcavity. Nano Hybrids, 2013, 3, 51-65.	0.3	Ο
198	Characterization of ZnO/Cu/ZnO multilayers structure for solar cell devices. AIP Conference Proceedings, 2016, , .	0.4	0

#	Article	IF	CITATIONS
199	Study of laser intensity on gold nano-particles preparation in a harsh environment. , 2016, , .		0
200	Ex-situ Generation of the Gold Nanowire Networks Bovine Serum Albumin Bio-Conjugated System Using Pulsed Laser Ablation in a Harsh Environment. Journal of Physics: Conference Series, 2018, 1083, 012011.	0.4	0
201	Synthesis of Architectural-Cubic Porous Silicon by Electroless Stain Etching in V2O5 and HF Solution. Silicon, 2020, 12, 1761-1768.	3.3	0
202	Structural and optical properties of ZnO nanoflakes/Al/glass via laser-assisted chemical bath deposition (LACBD) technique. Applied Physics A: Materials Science and Processing, 2021, 127, 1.	2.3	0
203	The Role of Alternating Current on Photo-Assisted Electrochemical Porosification of GaN. Journal of Nanoelectronics and Optoelectronics, 2014, 9, 287-290.	0.5	0
204	Structural, Electrical and Optical Properties of NiO Nanostructured Growth Using Thermal Wet and Dry Oxidation of Nickel Metal Thin Film. Journal of Nanoelectronics and Optoelectronics, 2018, 13, 628-636.	0.5	0
205	Challenges in Nanobiosensor Aiming Bioscience Applications. Nanotechnology in the Life Sciences, 2020, , 187-195.	0.6	Ο